

The Role of Neutral Beam Fueling Profile in the Performance of TFTR and other Tokamak Plasmas

H.K. Park, S.A. Sabbagh, S. Batha, M. Bell, R.V. Budny, C. Bush, Z. Chang, D. Johnson,
D.K. Mansfield, D. McCune, K.M. McGuire, R. Nazikian, C. Skinner, R. Wieland,
M. Yamada, and K.M. Young

Princeton Plasma Physics Laboratory, Princeton University, Princeton, NJ 08543

ABSTRACT

New scalings for the stored energy and neutron yield, determined from the experimental data are applied to both deuterium-only and deuterium-tritium plasmas at different operational domains in TFTR. The domain of the data considered includes the Supershot, High poloidal beta, L-mode, and limiter H-mode operational regimes, as well as discharges with a reversed magnetic shear configuration. The key parameter in this scaling is heating beam fueling profile shape. Energy confinement and neutron production are relatively insensitive to other plasma parameters compared to the beam fueling peakedness parameter and the heating beam power when considering plasmas that are stable to magnetohydrodynamic modes. The implication of the scalings based on this parameter is related to theoretical transport models such as E_r shear and ITG marginality models. Similar physics interpretation is provided for beam heated discharges on other major tokamaks.

I. Introduction

Among many scaling studies, the ITER-89P L-mode scaling [1] is well known and has been applied to most tokamaks around the world. While a high correlation with the chosen data has been achieved over the entire domain considered, significant improvements (and also degradations) have been produced in most tokamaks as compared to the scaling prediction. For example, in TFTR, a large variation of the stored energy [~ 0.5 to ~ 3.5 times that computed from the ITER-89P L-mode scaling as shown in Fig. 1a] for beam heated discharges has been produced. This observation has motivated the consideration of new independent variables to describe energy confinement and fusion power in TFTR. In particular, by introducing an independent variable related to the neutron beam fueling profile peakedness, we were able to produce a scaling with a smaller number of parameters and significantly reduced dispersion as shown in Fig. 1b.

It is demonstrated that the new scalings can be applied to all beam heated deuterium (D) discharges in TFTR such as L-mode discharges (whose confinement times fit the empirical L-mode scalings [2, 3]), the Supershot [4], High poloidal beta plasmas [5], discharges with a reversed shear (RS) magnetic configuration [6], limiter H-mode plasmas [7], and Supershots enhanced by Li pellet conditioning [8, 9]. These scalings were also applied to deuterium-tritium (DT) discharges. From the neutron scaling, one can estimate a scale factor between D and DT neutron yields. We find that the stored energy and neutron yield of TFTR neutral beam heated discharges are closely associated with the core fueling of the heating beams. We also find that the empirical relation between plasma ion energy content and the beam fueling parameter, H_{ne} , has a much different form than the relationship between electron energy content and the beam fueling parameter. The ion stored energy and fusion power production of the plasma can be relatively insensitive to variations in plasma current, I_p , toroidal field, B_T , and safety

factor, q , as compared to their dependence on H_{ne} . In contrast, the electron stored energy is relatively insensitive to H_{ne} , and has a greater dependence on plasma current. On the other hand, these plasma parameters are extremely important in determination of the stability boundary together with H_{ne} [10]. The role of H_{ne} in the performance has also been reported on other large neutral beam heated tokamaks [11, 12].

In section II, a brief summary of the modeled neutral-beam fueling profile shape factor [13] is provided. Here, the beam fueling profile shape factor is formulated as a function of plasma density and profile shape factor based TRANSP calculation. In section III, scalings with multiplication factors and exponents for the stored energy of each plasma species (ions and electrons) and the D neutron emission are provided. In section IV, further tests of the scalings for D discharges on new operating regimes such as Supershots at different major radii, enhanced Supershots with lithium conditioning, discharges with reverse shear magnetic configuration and DT discharges are discussed. Here, it is shown that the neutron production of discharges is not directly influenced by the toroidal field within the stability boundary where MHD activity is moderate [14]. In section V, we attempt to provide a connection of the scaling for ion stored energy to the key theoretical transport [15, 16, 17, 18] models. In the last section VI, the physics related with the beam fueling parameter in other major tokamaks based on published articles is reviewed.

II. Heating beam fueling profile

The definition as well as the detailed calculation of the computed neutral-beam particle deposition profile peakedness for TFTR are provided in Refs. [13, 19]. Following these studies, H_{ne} is defined as ratio of the central beam fueling rate to the volume averaged beam fueling rate. This definition is similar to the density peakedness factor

$F_{ne} = n_e(0) / \langle n_e \rangle$, where $n_e(0)$ is the central electron density and $\langle n_e \rangle$ is volume-averaged electron density. Note that H_{ne} is a similar definition to $H(0)$ established in the earliest days of neutral beam research [20]. When the beam has single energy component, $H_{ne} = H(0)$. The attenuation of the injected neutral-beam is to first order proportional to the local electron density, so a peaked neutral-beam deposition profile can be achieved at high density only with a peaked density profile in TFTR. In order to parameterize the expression of H_{ne} for a variety of discharges, a regression has been performed for values of H_{ne} calculated by the TRANSP code [21] as a function on line-averaged electron density and the density peakedness factor. Among the functional combinations, the best description is

$$H_{ne} = 2.41 F_{ne}^{1.04} \text{EXP}(-0.24 \times 10^{-19} \bar{n}_e), \quad [1]$$

and shown in Fig. 2, where F_{ne} and \bar{n}_e (in m^{-3}) are the measured peakedness and line-averaged density of electrons. The relationship in Eq. [1] shows that a peaked electron density profile shape is essential for peaked deposition of the neutral beam at high density. This expression (with the same coefficients) is applicable to TFTR discharges at different major radius. This subject is discussed in section V.

Using the measured $F_{ne}(t)$ and $\bar{n}_e(t)$, it is instructive to examine the time dependence of H_{ne} together with other plasma parameters for typical TFTR discharges. Fig. 3 shows the temporal evolution of H_{ne} for L-mode and supershot discharges for the same beam power ($P_B \sim 22$ MW). In the supershot, the initial central beam fueling is significantly greater than the L-mode plasma due to differences in the pre-beam electron density. The initial high level of central beam fueling is maintained in the Supershot ($H_{ne} \sim 3.0$) as \bar{n}_e is increased, until a "Carbon bloom" [22] (accompanied by a sudden rise of edge

electron density) occurs at about 3.8 sec. The degradation of W_{tot} and neutron emission (S_n) is well correlated with the reduction in H_{ne} (~ 3.0 to ~ 1.0). For the L-mode plasma, the low initial beam fueling ($H_{ne} \sim 1.0$) falls rapidly to ~ 0.3 so that subsequent to NBI, there is almost an order of magnitude difference in H_{ne} between the supershot and L-mode plasmas. It is striking, however, that the accumulated W_e in each discharge is similar in magnitude. Therefore W_i in the supershot discharge is significantly greater than that of the L-mode discharge. The D-D fusion neutron emission in the L-mode discharge is an order of magnitude smaller than that of the supershot discharge. The strong dependence of W_i on H_{ne} , and the relatively weak dependence on H_{ne} suggests that the two species should be considered separately when developing a scaling for total energy in TFTR.

III. Scalings for the stored energy and fusion reactivity

The study involves approximately 870 TFTR deuterium discharges, constrained to deuterium gas fueled discharges only. The data points consist of each plasma parameter at the time of the peak global stored energy. A wide range of beam power ($5 \text{ MW} < P_B < 32 \text{ MW}$) and plasma current ($0.9 \text{ MA} < I_p < 2.0 \text{ MA}$) are included. In all discharges, the beam power exceeds the Ohmic power by a factor of ~ 5 to reduce the influence of Ohmic heating on confinement. Deuterium beams with $90 \text{ keV} < E_{inj} < 110 \text{ keV}$ are injected tangentially and the data are restricted to nearly balanced injection, i.e., $|(P_{co} - P_{ctr}) / (P_{co} + P_{ctr})| < 0.4$, where the subscript co and ctr refer to injection in the same and opposite direction with respect to the plasma current, respectively. The total stored energy (W_{tot}) is determined from magnetic measurements, so that both the thermal and fast-beam ion energies are included. The electron stored energy, W_e , is calculated using the measured electron density and temperature profile. The ion stored energy W_i is defined as

($W_{\text{tot}} - W_e$). Note that W_i consists of both thermal and fast beam-ions. In principle, the stored energy of fast-beam ions should be studied separately from thermal ions. However, there is a problem in distinguishing thermal ions from fast-beam ions when the ion temperature, as inferred from the measured carbon impurity temperature, approaches the incoming beam-ion energy. Note that if the conventional analysis is applied to supershot plasmas [23], the fast-beam ion fraction in the supershot discharge is very close to that of an L-mode plasma. In order to eliminate other possible strong parametric dependencies, this data set is constrained to fixed plasma major and minor radii of $R = 2.45$ m, and $a = 0.8$ m, and toroidal magnetic field $B_T = 4.0$ T and 4.8 T.

The observed scatter in the ion stored energy data at various heating power can be significantly reduced by utilizing the parameters H_{ne} and I_P as shown in Ref. [10, 19]. Most importantly, the role of H_{ne} is much more significant than that of I_P . Thus the stored ion energy can be described well by using only P_B and H_{ne} as shown in Fig. 4 with the scaling

$$W_i(J) = C_1 P_B^{1.3} (MW) H_{ne}^{0.8}, \quad [2]$$

where C_1 is 2.04×10^4 . The fact that the stored ion energy scaling is nearly linearly correlated with the central beam fueling ($P_B H_{ne}$) has important implications. For a fixed H_{ne} , the heating beam power dependence is quite different from the conventional L-mode scaling ($P_B^{0.5}$). Note that the power dependence in Eq. 2 is applicable to all the discharges in TFTR; sub-L-mode discharges, L-mode discharges, discharges, Supershots, lithium enhanced Supershots, and discharges with different magnetic configurations. Comparisons with recent theoretical transport models will be given in a later section.

The parametric dependence of the electron stored energy is significantly different from that of the ion stored energy. The result is given as

$$W_e(J) = C_2 P_B^{0.7} (MW) I_p^{0.4} (A), \quad [3]$$

where C_2 is 310. While H_{ne} is important in the determination of the ion stored energy, it is not important in the determination of the electron stored energy. It is interesting to find that the parametric dependence of stored energy of electrons is characteristically similar to L-mode scaling. Note that the fraction of electron stored energy is rapidly changing from 0.75 to 0.35 as the performance is improved. This may explain why the plasma current was not as important in Supershot regime as the L-mode scaling would indicate. The total stored energy of beam heated discharges can be defined simply as

$$W_{tot}^P = W_i + W_e. \quad [4]$$

In TFTR, the neutron emission rate, S_n , from DD reactions has a positive correlation near unity with the ion stored energy ($S_n \propto W_i^{1.6}$) as shown in Fig. 5. This result can be understood based on the reaction argument. The fusion cross-section ($\langle \sigma v \rangle$) is proportional to $\sim T_i^2$ for the range of ion temperatures (10 keV \sim 20 keV) on TFTR. Since the neutron yield is not entirely due to the thermonuclear reaction, the dependence is expected to be less than square. Note that in Supershots the neutrons from beam-target and beam-beam reactions are comparable to the neutrons from thermonuclear reactions. Using the same set of independent parameters employed in the study of energy confinement, the scaling result for the fusion reactivity is

$$S_n^P = C P_B^{2.2} (MW) H_{ne}^{1.3} / V_p (m^3), \quad [5]$$

where C is 2.71×10^{14} and V_p is plasma volume.

Furthermore, we can define the fusion power gain for DD discharges, Q_{DD} , for a fixed plasma volume as

$$Q_{DD} = S_n^p / P_B = C P_B^{1.2} (MW) H_{ne}^{1.3}. \quad [6]$$

As shown in this equation, Q_{DD} is nearly linear to the central beam fueling. Therefore, it is most efficient to improve Q_{DD} by increasing H_{ne} for a given heating beam power.

V. FURTHER APPLICATION OF THE SCALINGS ON TFTR

As limiter conditioning techniques have been developed using lithium pellets [9, 10], most of the recent D and DT discharges were operated at a larger major radius ($R_0 = 2.52$ m, $V_p = 37$ m³). This has produced enhanced Supershot discharges with energy confinement times up to 330 msec [9]. Note that the high energy confinement time obtained with lithium wall conditioning is almost twice that of the highest energy confinement time of the data base studied. In addition to these high performance discharges, an L-mode study was also recently performed with both D and DT plasmas with beam heated discharges at an even a larger major radius ($R_0 = 2.62$ m, $V_p = 46$ m³). This data set includes discharges with a reversed shear (RS) magnetic configuration [6].

We find that the major radius is not strongly correlated with the stored energy explicitly. This is illustrated in Fig. 6a, where the ratio (W_{tot} / W_{tot}^p) is shown as a function of heating beam power for discharges at three different major radii. Fig. 6b

illustrates that D discharges (Li enhanced Supershot discharges, Supershot, and L-mode) fit reasonably well with the scaling ($W_{\text{tot}}^{\text{P}}$). Discharges (~150 shots) with reversed shear (RS) magnetic configuration fit well with $0.8 \times W_{\text{tot}}^{\text{P}}$ as shown in Fig. 7a. When neutron production was examined for discharges with the RS configuration, the result was $0.65 \times S_{\text{n}}^{\text{P}}$, which is consistent with the prediction based on the self-consistent relationship between neutron production and stored energy discussed in the previous section. The central beam fueling is exceptionally good for some discharges with ERS configuration but the stored energy and fusion reactivity are well below the level of Supershot discharges if the same logistics on confinement and fusion reactivity are applied. The result may provide insight for future studies examining the role of the current profile shape on plasma confinement.

The initial DT experiments [²⁴, ²⁵] on TFTR showed that the stored energy of DT discharges is about 25% higher than that of comparable D discharges. This fact has been attributed to an isotopic effect [23] due to the usage of tritium. When the scaling ($W_{\text{tot}}^{\text{P}}$) of the stored energy derived from D discharges is applied to DT plasmas, it is found that the stored energy of DT discharges (both supershots and L-mode discharges) fits to $1.25 \times W_{\text{tot}}^{\text{P}}$ as shown in Fig. 8a. Note that the DT discharges in this figure have a fuel ratio (T/(D+T)) ranging from 30% to 70%. Considering that there are many differences between deuterium and tritium beam sources as discussed in section 2, it would be desirable to have a comparison study of ohmic deuterium and tritium plasmas where the energy of the neutral of D and T are identical, in order to clarify whether or not this difference is due to an intrinsic isotopic effect in the plasma rather than due to the heating beam sources.

VI. Relationship to theoretical transport models

There have been many different theoretical models proposed to explain variations in E in tokamaks. These efforts can be divided into two groups; localized enhanced core transport based on ExB shear [18], and non-local enhanced core transport based on ITG marginality [15].

Transport models based on radial electric field shear, inherited from the interpretation of L to H transition at the plasma edge may be explicitly related to the physics basis of the beam fueling peakedness. Experimentally, the beam fueling profile is clearly instrumental for the control of pressure profile via the ion channel as shown in Eq. 2. The p_i controlled by H_{ne} can be the source of the radial electric field in the transport theory where toroidal plasma rotation is small. In fact, the theoretical models require a justification for the usage of steep pressure gradient as a driving source. Since the central beam fueling is experimentally responsible in the determination of the ion stored energy, as we have learned in the previous section, it may provide the theoretical physics mechanism that can suppress the turbulence and hence improving the confinement. Even though this model is not constrained by particular wall recycling conditions, a high central plasma pressure can only be driven by high H_{ne} in TFTR. This requires a low edge density or good wall conditioning. This requirement of low edge density condition can be significantly relaxed when plasma shaping is introduced simply due to geometric effect for a tokamaks equipped with on axis beam injection system.

The non local nature of core transport model based on ITG marginality is associated with the edge plasma conditions. This model has many common features with confinement scaling based on H_{ne} , even though this parameter is not explicitly used in this model. Since the high edge ion and electron temperatures are key elements in this model, high central beam fueling is expected in TFTR in low recycling conditions when the edge temperature is high and the edge density is low. This in turn results in a peaked

density profile in NB heated plasmas. The peaked density profile leads to increased confinement in both the model and scaling.

It is important to note that a peaked electron density profile alone is not a sufficient condition to improve the stored plasma energy in beam heated discharges in TFTR. Beam heated discharges with highly peaked density profile at extremely high line-averaged density produced by solid D pellet did not improve with respect to L-mode confinement time. This result is consistent with the corresponding exponential decrease of H_{ne} [Eq. 1] at sufficiently high density. A recent significant improvement in energy confinement and neutron production created by intense wall conditioning using Li-pellet injection [8, 9] prior to the injection of the beam, can be examined with the same logistics.

VI. The role of beam fueling profile in the performance of other tokamaks

In the previous sections, we have demonstrated that a significant variation of energy confinement in TFTR with respect to ITER-89P L-mode scaling (which has been used as a basis of the ITER design), can be reduced substantially with the scaling based on beam fueling peakedness. If this observation is a universal phenomena, would not be surprising to find similar effects of H_{ne} on the performance of beam heated discharges in other tokamaks as shown in Refs [11,12]. Even though, the neutral beam heating sources used in most tokamaks are more or less similar to the beam sources employed in TFTR, there are significant differences in the beam fueling profile due to the beam line arrangement and operating plasma positions. In addition to the differences in engineering configuration, the time evolution of plasma density profiles can influence the dependence of the performance on H_{ne} .

It has been known that shaped and diverted plasmas differ from circular plasmas, since the profiles are generally to be broader and the stability limits larger. Due to the relatively small contact point of the divertor strike point with the wall, there is a distinctive advantage in the particle influx control. However, it is surprising to find that there are similarities in the performance improvement in a diverted plasma with respect to the beam fueling. For instance, the fusion power gain for beam heated discharges in JET is shown to be $Q_{DD} = P_B(\text{central})$ [11] which can be qualitatively interpreted as the derived result for TFTR (Eq. [6]).

The NBI systems on the JET tokamak are equipped with two different beam energies (~ 140 keV and ~ 80 keV) and allow on-axis tangential injection. However, recent modifications implemented for a divertor study have resulted in an off-axis tangential heating system due to the imposed upward shift of the plasma position. This may not be entirely responsible for the observed degraded performance following the installation of the new divertor system but it provides a logical interpretation of the result [26]. Differences in the beam fueling profile might also help explain the result that the plasmas with an increased triangularity on JET did not improve performance [26] whereas similar experiments in DIII-D yielded improved performance [27]. In JET case, increased triangularity implies that the central beam fueling is further degraded, however the result is opposite in DIII-D. Also elongation (from $\kappa = 1.68$ to $\kappa = 1.94$) experiments in DIII-D showed improved energy confinement together with increased H_{ne} [28]. The DIII-D tokamak has a tangential injection system with a beam energy of approximately ~ 80 keV. Furthermore, the recent high fusion gain results [29] from DIII-D suggests that the peakedness of the beam fueling (90 % central beam fueling) may be responsible for the enhanced fusion reactivity. The "L-mode edge" discharges with increased H_{ne} have produced significantly enhanced neutron rates compared broader profile VH modes (a

factor of ~ 5) with the same heating beam power. Note that the neutron yield of the former discharges is comparable to the level of TFTR for similar heating beam power and H_{ne} .

The JT-60U tokamak is equipped with a flexible but mainly off-axis heating system for full size plasma ($V_p = 100 \text{ m}^3$) operation with a beam energy of approximately $\sim 90 \text{ keV}$. On JT-60U, the discharges with the best performance have been created in the high poloidal beta, β_p , regime obtained when a relatively small plasma ($V_p = 37 \text{ m}^3$) was formed toward the high field side of the vacuum vessel. This confirmation allows central beam fueling in the JT-60U plasma [30]. Note that the beam deposition is always hollow for a full size plasma on JT-60U. Although a successful initial attempt was made to unify results [17] between TFTR Supershot and JT-60U high β_p regimes based on beam fueling profile shape, lack of reliable density information in the JT-60U high β_p regime and possible intrinsic differences between divertor and limiter plasmas requires more careful study.

VII. SUMMARY

Scalings of the ion and electron energy, and neutron yield have been derived for TFTR beam heated plasmas which include L-mode, limiter H-mode, Supershot, high β_p , and reversed shear confinement regimes in TFTR. An important feature of this scaling study is the substantial reduction of the number of independent variables required to produce a good fit to the data. This is made possible by the inclusion of an independent variable that models the peakedness of the beam fueling deposition profile. The ion and electron components of the plasma are separately analyzed. The ion stored energy is sensitive to the central beam fueling. The electron stored energy is found to be insensitive to H_{ne} and a dependence on plasma current is observed. Scalings with fixed multiplication factors and exponents for the stored energy and neutron yields were

applied to both D and DT discharges at different major radius with various wall conditions. Beam fueling peakedness plays an important role in transport models that incorporate ion pressure gradient term (such as EXB shear model). The edge condition required for TFTR to increase H_{ne} is consistent with the edge condition needed for improved confinement in the ITG marginality model. The importance of beam fueling parameters are also evident in other major tokamak plasmas.

ACKNOWLEDGMENT

This work was supported by U.S. DoE contract No. DE-ACO2-76-CH03073 and DE-FG02-89ER53297. We would also like to thank Drs. R. Hawryluk and D. Meade for the support of this work.

Figure Captions

Figure 1. (a) Measured stored energy for TFTR beam-heated plasmas is compared with that of the ITER 89P L-mode scaling. The range spans from 0.5 to 3.5 times that of ITER 89P L-mode scaling. (b) Measured stored energy for TFTR beam-heated plasmas is compared with that of the new scaling. The dispersion is reduced significantly. Here, DT discharges and reverse sheared discharges are multiplied by 1.25 and 0.8, respectively.

Figure 2. The beam fueling parameter is formulated as a function of line average density and profile shape. H^{TRANSP} is calculated beam fueling peakedness from TRANSP.

Figure 3. The temporal evolution of H_{ne} based on Eq. 1 with other plasma parameters such as global stored energy (W_{tot}), stored energy of electrons (W_e), and line average density for the same heating-beam power ($P_B \sim 22$ MW); Solid --- - "supershot"

discharge at $I_p = 1.4$ MA and dotted --- - L-mode discharge at $I_p = 2.0$ MA. Average H_{ne} value of the supershot is an order of magnitude higher than that of L-mode for the first half second.

Figure 4. The influence of H_{ne} on the ion stored energy is demonstrated for beam heated discharges. The ion stored energy is nearly a linear function of the central beam fueling parameter ($P_B^{1.3} H_{ne}^{0.8}$).

Figure 5. The measured DD fusion neutron emission (S_n) has a tight correlation with $CW_i^{1.6}$. Deviation from a square dependence can be attributed to the importance of beam target and beam-beam reactions in addition to the thermonuclear reaction.

Figure 6. (a) The ratio (W_{tot}/W_{tot}^P) is depicted as a function of heating beam power for discharges at three different major radius. (b) Comparison of the measured and modeled W_{tot} for D discharges at various operating conditions (Li-enhanced Supershots, Supershots, L-mode).

Figure 7. Discharges with RS magnetic configuration obtained at $R_O = 2.62$ m are compared with W_{tot}^P . The best fit is $0.8 \times W_{tot}^P$.

Figure 8. The measured stored energy of DT discharges (supershots and L-mode discharges) with a mixture ranging from 30 % to 70 % is compared with $1.25 \times W_{tot}^P$.

Multiplier 1.25 is attributed to the isotopic effect from the usage of tritium.

[1] Yushmanov, P.N., Takezuka, T., Riedel, K.S., et al., Nuclear Fusion **30** (1990) 1999

[2] Goldston R.J., Plasma Phys. **26** (1984) 87.

[3] Rebut, P.H., Lallia, P.P., Watkins, M.L., in Plasma Physics and Controlled Nuclear Fusion Research 1988 (Pro. 12th Int. Conf. Nice, 1988), Vol.2, IAEA, Vienna (1989)

191.

[⁴] Strachan, J., Bitter, M., Ramsey, A.T., Zarnstorff, M.C., et al., Phys. Rev. Lett. **58** (1987), 1004.

[⁵] Sabbagh, S.A., Gross, R.A., Mauel, M.E., et al., Phys. Fluids B **3** (8), (1991), 2277.

[⁶] Levinton, F., Zarnstorff, M.C., Batha, S.H., et al., Phys. Rev. Lett. **75** (1995), 4417.

[⁷] C. E. Bush, et al., Phys. Rev. Lett. **65** (1990) 424.

[⁸] Mansfield, D.K., Strachan, J.D., Bell, M.G., et al., Phys. of Plasmas **2** (1995), 4252.

[⁹] Mansfield, D.K., Hill, K.W., Strachan, J.D., et al., Phys. of Plasmas **3** (1996), 1.

[¹⁰] Park, H.K., and Sabbagh, S.A., submitted in Nuclear Fusion 1996

[¹¹] Thompson, E., Stork, D., de Esch, H.P.L., and the JET Team, Phys. Fluids B **5** (7), (1993) 2468.

[¹²] Park, H.K., Bell, M., Ishida, S., et al., in Proceedings of the 15th International Conference on Plasma Physics and Controlled Nuclear Fusion Research, (Seville, Spain, 1994), (International Atomic Energy Agency, Vienna, Austria) Vol. **1** (1995) 211.

[¹³] Park, H.K., et al., Nucl. Fusion, **32** (1992) 1042.

[¹⁴] Chang, Z, Fredrickson, E.D., Callen, J.D., et al., Nucl. Fusion **34** (1994) 1309.

[¹⁵] Kotschenreutor, M., Dorland, W., Beer, M.A., Hammett, G.W., Phys. Plasmas **2** (1995) 2381.

[¹⁶] Beer, M.A., Hammett, G.W., et al., to appear in Phys. Plasmas (1996).

[¹⁷] Drake. J.F., et al., Phys. Rev. Lett. **77** (1996) 494.

[¹⁸] Itoh, S.I. and Itoh, K.J., J. Phys. Soc. Jpn. **59** (1990) 3098.

[¹⁹] Park, H.K., M.G. Bell, W.M. Tang, G. Taylor, M. Yamada, Nucl. Fusion, **34** (1994) 1272

[²⁰] Rome, J.A., Callen, J.D., Clarke, J.F. Nucl. Fusion **14** (1974) 141.

[²¹] Budny, R.V., Nucl. Fusion, **34** (1994), 1205.

[²²] Ramsey, A.T., et al., Nuclear fusion **31**, (1991) 1811

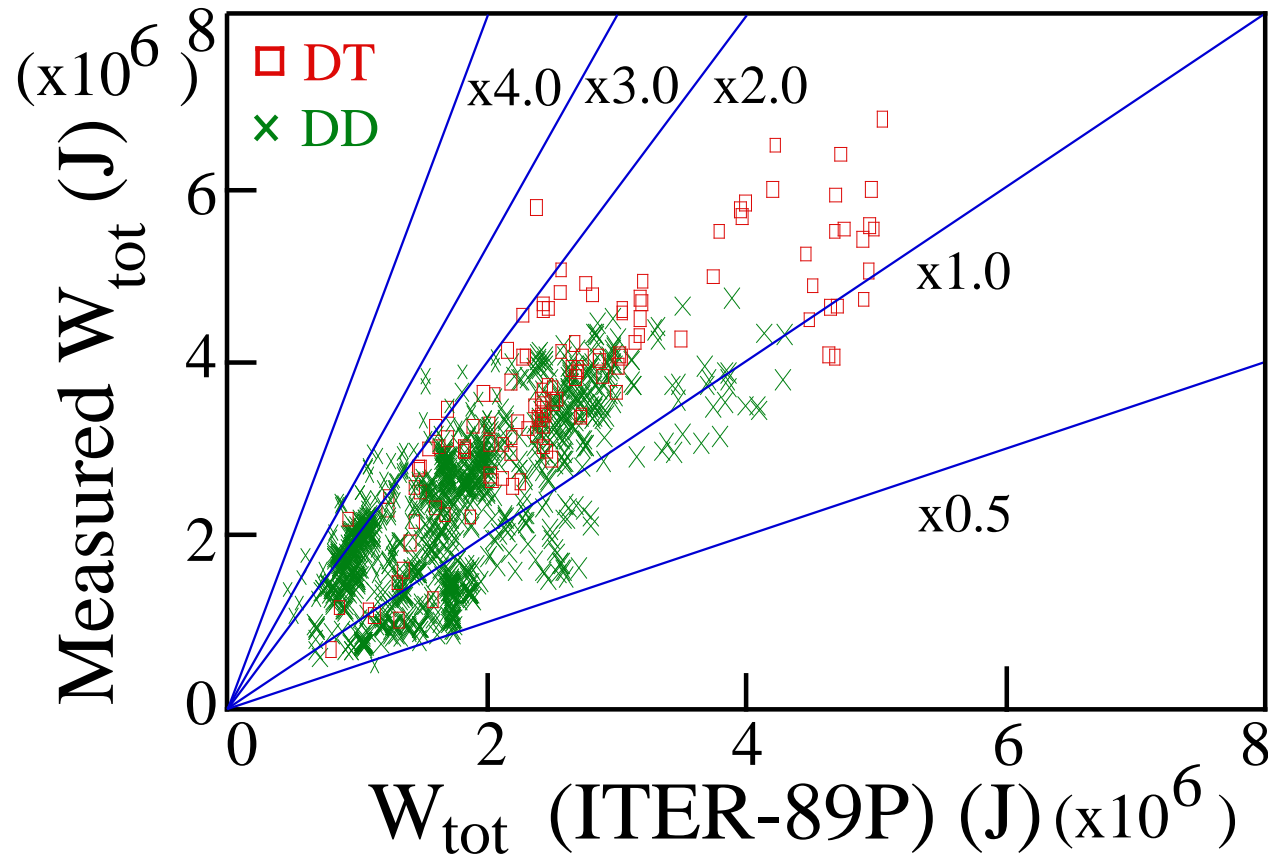
[²³] Scott, S.D., et al., Phys. Fluids **B 2** (1990) 1300.

[²⁴] Strachan, J.D., Adler, H., Alling, P., et al., Phys. Rev. Lett., **72**, (1994), 3526.

-
- [²⁵] Hawryluk, R.J., Adler, H., Alling, P., *et al.*, Phys. Rev. Lett., **72**, (1994), 3530
- [²⁶] JET Team, in Proceedings of the Fifteenth International Conference on Plasma Physics and Controlled Nuclear Fusion Research, (Seville, Spain, September/October 1994), (International Atomic Energy Agency, Vienna, Austria) Vol. I, 211, Paper IAEA-CN-60/A2-4
- [²⁷] Lazarus, E., *et al.*, in Proceedings of the Fifteenth International Conference on Plasma Physics and Controlled Nuclear Fusion Research, (Seville, Spain, September/October 1994), (International Atomic Energy Agency, Vienna, Austria) Vol. I, 31, Paper IAEA-CN-60/A1-2
- [²⁸] Greenfield, C.M., DeBoo, J.C., Osborne, T.H., *et al.*, Bull. of APS, 36th Annual meeting of the Division of Plasma Physics, paper 5P2, (1994) 1644
- [²⁹] Rice, B.C., Bull. of APS, 37th Annual meeting of the Division of Plasma Physics, 1995, to be published in Phys. of Plasma.
- [³⁰] JT-60U Team, in Proceedings of the Fifteenth International Conference on Plasma Physics and Controlled Nuclear Fusion Research, (Seville, Spain, September/October 1994), (International Atomic Energy Agency, Vienna, Austria) Vol. I, 31, Paper IAEA-CN-60/A1-2

Motivation Significant Deviation from L-mode Scaling

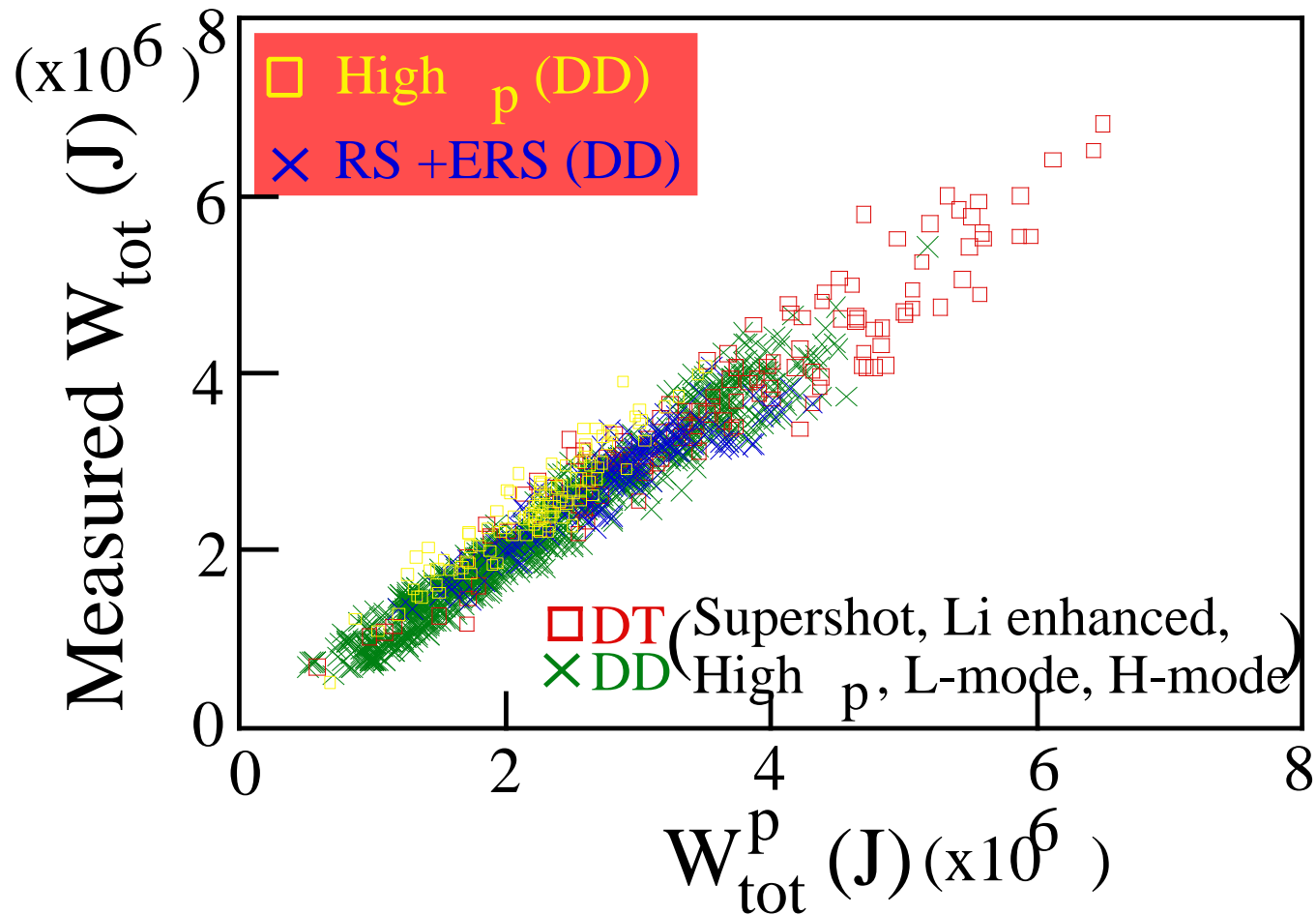
- Factor of ~ 7 variation in stored energy in TFTR
- Similar diversity observed in other tokamaks



$$(I_P^{0.85} P_B^{0.5} R^{1.2} a^{0.3} n_e^{0.1} B_T^{0.2} M^{0.5})^{0.5}$$

Improved correlation achieved with new W_{tot} scaling

- Key independent parameter: beam fueling profile peakedness (H_{ne})

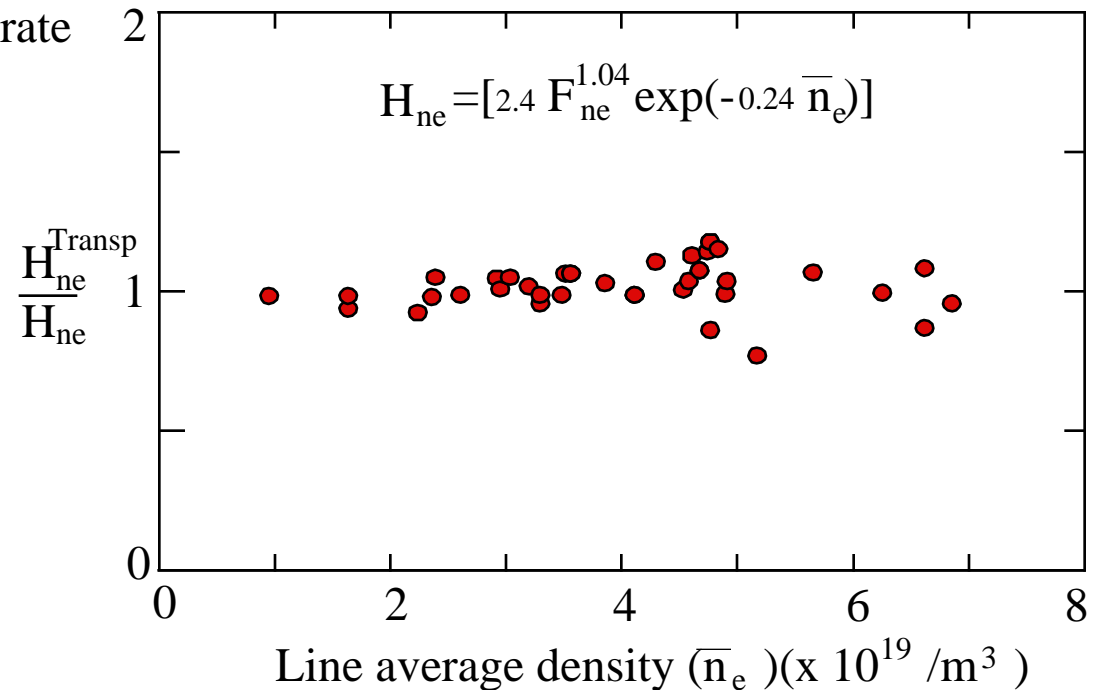
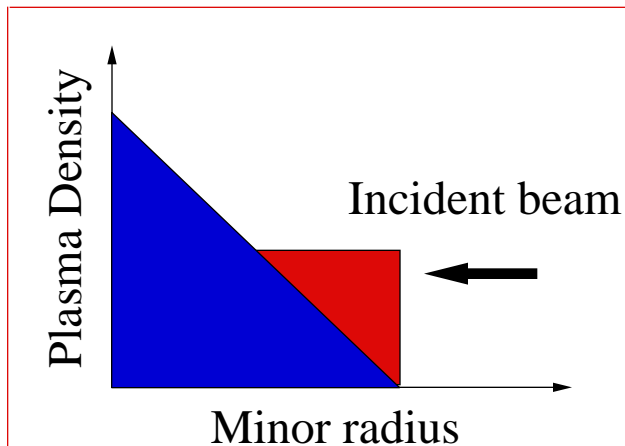


$$\left(2.04 \times 10^4 P_B^{1.3} H_{\text{ne}}^{0.8} + 310 P_B^{0.7} I_P^{0.4} \right)$$

(Ions)
(Electrons)

Beam Fueling peakedness is modelled as a plasma density and density profile shape

$$H_{ne} = \frac{\text{Central beam fueling rate}}{\text{Volume average beam fueling rate}}$$

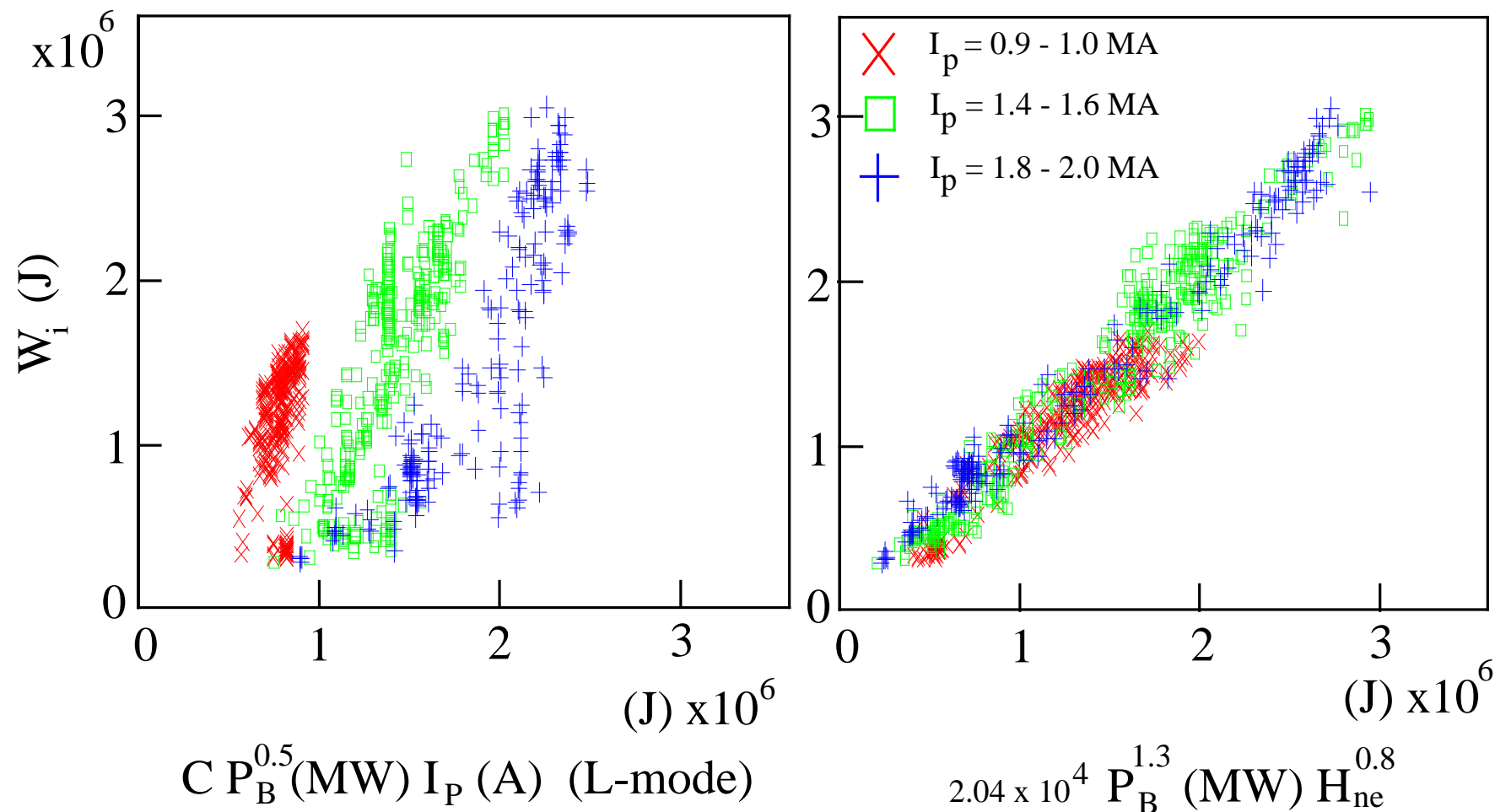


■ H_{ne}^{Transp} : TRANSP calculated beam fueling peakedness

■ H_{ne} : Modelled as $H_{ne} = F_{ne} \exp(-\bar{n}_e)$

\bar{n}_e = line average density, $F_{ne} = n_e(0) / \langle n_e \rangle$.

Ion Stored Energy Scaling is Approximately Linear in H_{ne}



- Scaling for electron stored energy is independent of H_{ne}

$$W_e \text{ (J)} = 310 P_B^{0.7} \text{ (MW)} I_P^{0.4} \text{ (A)}$$